



Criteria for selection of components for surrogates of natural gas and transportation fuels [☆]

Hongzhi R. Zhang ^{*}, Eric G. Eddings ¹, Adel F. Sarofim

Department of Chemical Engineering, The University of Utah, Salt Lake City, UT 84112, USA

Abstract

The present paper addressed the production of soot precursors, acetylene, benzene and higher aromatics, by the paraffinic (*n*-, *iso*-, and *cyclo*-) and aromatic components in fuels. To this end, a normal heptane mechanism compiled from sub-models in the literature was extended to large *normal*-, *iso*-, and *cyclo*-paraffins by assigning generic rates to reactions involving paraffins, olefins, and alkyl radicals in the same reaction class. Lumping was used to develop other semi-detailed sub-models. The resulting mechanism for components of complex fuels (named the Utah Surrogate Mechanism) includes detailed sub-models of *n*-butane, *n*-hexane, *n*-heptane, *n*-decane, *n*-dodecane, *n*-tetradecane and *n*-hexadecane, and semi-detailed sub-models of *i*-butane, *i*-pentane, *n*-pentane, 2,4-dimethyl pentane, *i*-octane, 2,2,3,3-tetramethyl butane, cyclohexane, methyl cyclohexane, tetralin, 2-methyl 1-butene, 3-methyl 2-pentene and aromatics. Generic rates of reaction classes were found adequate to generate reaction mechanisms of large paraffinic components. The predicted maximum concentrations of the fuel, oxidizer, and inert species, major products and important combustion intermediates, which include critical radicals and soot precursors, were in good agreement with the experimental data of three premixed flames of composite fuels under various conditions. The relative importance in benzene formation of each component in the kerosene surrogate was found to follow the trend aromatics > *cyclo*-paraffins > *iso*-paraffins > *normal*-paraffins. In contrast, acetylene formation is not that sensitive to the fuel chemical structure. Therefore, in formulation of surrogate fuels, attention should be focused on selecting components that will yield benzene concentrations comparable to those produced by the fuel, with the assurance that the acetylene concentration will also be well approximated.

© 2006 The Combustion Institute. Published by Elsevier Inc. All rights reserved.

Keywords: Kerosene reaction mechanism; Gasoline reaction mechanism; Natural gas reaction mechanism; Transportation fuel surrogate; Soot precursor formation

1. Introduction

The present paper is directed at the development of kinetic mechanisms for predicting the

concentration of the soot precursors acetylene and benzene in surrogate mixtures representing liquid transportation fuels. Liquid transportation fuels are mixtures of paraffins (*normal*-, *iso*-, and *cyclo*-), and aromatics. Previous combustion studies of surrogate formulations for transportation fuels include a fuel-rich premixed flame of kerosene composed of 79% paraffins, 10% *cyclo*-paraffins, and 11% aromatics studied by Vovelle and co-workers [1]; premixed flames of two gasoline fuels approximately 60% of

[☆] Supplementary data for this article can be accessed online. See Appendix A.

* Corresponding author. Fax: +1 801 585 5607.

E-mail address: westshanghai@yahoo.com (H.R. Zhang).

¹ Presenting author.

which were paraffins by Hakansson and co-workers [2].

Kinetic mechanisms have been assembled from the literature and extended for the *normal*-, *iso*-, and *cyclo*-paraffins to form the Utah Surrogate Mechanism [3]. Because of space limitations, the extension of the mechanisms to be discussed here are limited to those of large *normal*-, *iso*-, and *cyclo*-paraffins that are major components of transportation fuels and also found in minor amounts in natural gas [4].

The widely studied heptane reaction set [5,6] is often used as a building block for mechanisms of higher paraffins. A lumping procedure for the detailed kinetic models was well described in the excellent review by Ranzi et al. [7]. The present paper emphasizes flame studies, drawing on previous experimental and numerical studies of higher paraffins: by Bales-Gueret, Cathonnet, Dagaout and co-workers on the oxidation of *n*-decane [8,9] and kerosene [10] in jet stirred reactors; by Vovelle and co-workers on *n*-decane [11] and kerosene [12] fuels diluted with argon in both a jet-stirred reactor at a pressure of 6000 Pa and in atmospheric flames [13]; by Fournet et al. [14] on the combustion of *n*-hexadecane in a well-stirred reactor at three different equivalence ratios; and the numerical studies of larger paraffin components in liquid transportation fuels by Battin-Leclerc and co-workers [15,16] who applied an automatically generated mechanism with 7920 reactions to a JSR experiment and a premixed flame; by Kyne and co-workers [17] to model a JSR experiment, a premixed flame and several counter-flow diffusion flames, with a kerosene surrogate composed of 89% *n*-decane and 11% toluene; by Mawid and co-workers [18] on modeling the ignition data for *n*-decane; by the development of mechanisms of *n*-decane [12,19,20] guided and validated by the data in the Vovelle experiments [11,13] mentioned above.

The numerical accuracy in predicting concentrations of larger olefins plays an important role in combustion modeling since these species are among the first intermediates formed from the decomposition of large paraffins, mainly via β scission, and the deviations of their concentrations may propagate to smaller olefins, via hydrogen addition reactions followed by β scission of large olefins. Also larger olefins are important sources of allylic radicals formed via thermal decomposition; allylic radicals determine the concentrations of many important aromatic precursors such as propyne, butyne, butene isomers and most unsaturated species that constitute major formation routes for benzene [3]. The emphasis of the mechanism development in the present study for combustion of composite fuels is therefore on reactions that involve the evolution of soot precursors, such as olefins and other unsaturated species, and the formation of

benzene, in addition to the fuel consumption and the formation of major products. The above reactions form the basis for correctly identifying major benzene formation pathways in flames with composite fuels based on the chemical structure of the individual fuel species.

2. Experimental data, reaction model, and surrogate formulation

The mechanism is based on that of *n*-heptane [3], which is extended to include more than two dozen sub-models of olefins, tetralin, C₄–C₁₆ paraffins and aromatics. The extended mechanism (Utah Surrogate Mechanism) was previously used to model premixed flames of *n*-heptane [21] ($P = 760$ torr, $\Phi = 1.0$ and 1.9), iso-octane [3] ($P = 760$ torr, $\Phi = 1.9$), *n*-decane [21] ($P = 760$ torr, $\Phi = 1.7$), cyclohexane [22] ($P = 30$ torr, $\Phi = 1.0$), and a PSR experiment of *n*-hexadecane [21] ($P = 760$ torr, $\Phi = 1.5$). In the current study, the extended mechanism is used to model three premixed flames burning composite fuels of kerosene [1] ($P = 760$ torr, $\Phi = 1.7$), gasoline [2] ($P = 760$ torr, $\Phi = 1.0$) and natural gas [4] ($P = 40$ torr, $\Phi = 1.0$). The kinetic simulation tool used for this study is CHEMKIN IV [23].

Surrogate formulation is one of the most important aspects necessary to achieve numerical accuracy in predicting the flame structure of a complex composite fuel. A surrogate is usually formulated to match the chemical and physical characteristics of the real fuel, by representation of the fractions of different chemical families, by use of an equivalent chemical formula, or by use of the functional groups in the composite mixture [24], with the composition adjusted to meet certain objective functions (e.g., ignition, sooting tendency, and fuel stability) and constraints (simplicity, cost of components). Ranzi and co-workers [25] suggested a surrogate for the kerosene flame [1] that satisfies the chemical composition constraints of the fuel, and includes 73.5% *n*-dodecane, 5.5% iso-octane, 10% methyl cyclohexane, 10% toluene and 1% benzene. The surrogate can be represented by an equivalent chemical formula of C_{10.72}H_{22.36} and will be adopted in this work. Turbiez et al. [4] measured the flame structure of a synthetic natural gas, which consisted of 88.4% methane, 9.52% ethane, 1.84% propane, 0.09% *n*-butane, 0.07% *iso*-butane, 0.05% *n*-pentane, 0.05% *iso*-pentane and 0.05% *iso*-hexane. A surrogate of 22 components, a close approximation to the fuel, will be used to simulate the European Unleaded Certified Gasoline flame [2] including 1.7% (in volume) *n*-butane, 15% *iso*-pentane, 3.4% *n*-pentane, 4.8% *iso*-hexane, 2.6% *n*-hexane, 1.4% benzene, 8.6% cyclohexane, 10.1% toluene, 4.4% 2,4-dimethyl pentane, 1.0% *n*-heptane, 10.6% iso-octane, 2.6% 2,2,3,3-tetramethyl butane, 13.7% xylenes, 2.5%

ethyl benzene, 5.5% methyl ethyl benzene, 5.5% propyl benzene, 3.0% methyl styrene, 1.1% ethyl naphthalene, 0.8% 2-methyl 1-butene, 0.7% 1-pentene, and 1.0% 3-methyl 2-pentene.

3. Mechanism generation of paraffin species

The basics of normal paraffin consumption in flames (see e.g. [7,12,21]) involve either thermal decomposition or hydrogen abstraction to form alkyl radicals, each of which decomposes via β scission to form one smaller alkyl radical and one olefin. Therefore with reliable sub-mechanisms of olefins and alkyl radicals, the normal paraffin decomposition can be described by a cascading decomposition chemistry of olefins and alkyl radicals of homologous series, as illustrated by the shaded area in Fig. 1. The methodology can be easily extended to the mechanism generation of *iso*- and *cyclo*-paraffins.

Major reaction classes that involve paraffins, olefins, and alkyl radicals in the extended mechanism are assigned similar rates with adjustments for different reaction sites; the generic rates of these reactions are summarized elsewhere [21]. These reactions in mechanisms of large paraffins include fuel consumption routes via hydrogen abstraction and thermal decomposition reactions, as well as other subsequent reactions to consume the direct intermediates from the fuel decomposition. Generic rates are not assigned to reactions that involve alkynes, allylic radicals, and other unsaturated species due to the paucity of the literature for these reactions. However, rates of those reactions were carefully estimated [3] by consulting findings in the literature for the same or similar reactions with adjustments in the statistical factor and activation energy. Only a few of these reactions need to be reevaluated during the mechanism generation of large paraffin sub-mechanisms since they involve mostly smaller species.

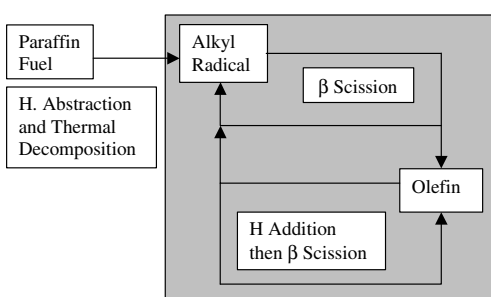


Fig. 1. The decomposition of normal paraffins can be presented as a collection of cascading decomposition sub-mechanisms of homologous series of olefin species and alkyl radicals.

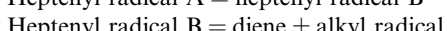
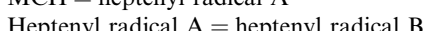
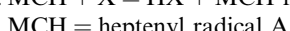
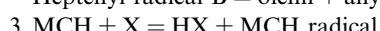
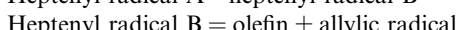
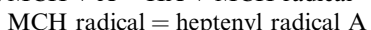
Thermal decomposition involves C–C σ bond cleavage only, and decomposition reactions are assumed similar except for those forming C_2H_5 and CH_3 radicals. For example, in reactions forming the methyl radical, the energy barrier is increased by 14.6 kJ/mol since CH_3 is the least stable alkyl radical. Hydrogen abstraction involves five different abstractors, which include H, OH, O, CH_3 , and O_2 . In detailed sub-mechanisms, all conjugate alkyl radicals formed from hydrogen abstraction of the fuel are included to account for the fuel decomposition more accurately.

Reactions of isomerization, β scission, and hydrogen abstraction by O_2 describe the chemistry of alkyl radicals in detail. Alkyl radicals convert to each other via isomerization. Reactions via a transition state of a six-membered intra-molecular ring of carbon and hydrogen atoms are preferred and given an energy barrier 16.7 kJ/mol lower than those of other isomerization reactions. Those from primary to secondary radicals are also favored by a decrease of 12.6 kJ/mol in the energy barrier due to the less stable nature of the former. Alkyl radicals decompose via β scission forming olefins with the double bond at the end of the carbon string. Conjugate olefins of the fuel are formed mainly via hydrogen abstraction by O_2 . Isomers of conjugate olefin are lumped into one species to reduce the model size, and the pre-factors of reaction rates involving these isomers are adjusted accordingly.

Olefins are consumed via hydrogen addition followed by β scission (major) and thermal decomposition (minor) to form allyl radicals. The consumption of smaller olefins and alkyl radicals formed in larger paraffin decomposition is added in the extended mechanism using generic rates. Reactions of olefins and alkyl radicals with seven carbons or less were already included in the base mechanism of *n*-heptane.

Lumping techniques have been used in the generation of the sub-mechanisms of *iso*- and *cyclo*-paraffins. For example, the sub-model of methyl cyclohexane (MCH) is built by collecting reaction routes that have proven to be important for normal paraffins. Like normal paraffins, *iso*- and *cyclo*-paraffins decompose mainly via hydrogen abstraction that is surpassed in importance by thermal decomposition only at high temperatures. Hydrogen abstraction and subsequent β scission reactions of conjugate alkyl isomers, however, are combined into one composite step; for example a typical reaction in the MCH sub-mechanism represents one of the following scenarios, which include three to four elementary steps:

1. $MCH + X = HX + MCH$ radical
- MCH radical = heptenyl radical
- $Heptenyl$ radical = olefin + allylic radical



Only the most powerful hydrogen abstractors in flames, H and OH radicals, are included in lumped reactions. The composite reactions are assigned generic rates of hydrogen abstraction at secondary carbon sites, by assuming that the hydrogen abstraction is the controlling step and that the following β scission is much faster. The conjugate species of the fuel from hydrogen abstraction sometimes undergoes isomerization, which is assumed instantaneous, before further decomposition. Only isomerization reactions via a transition state ring consisting of five-seven atoms are included. Thermal decomposition reactions, which are assigned generic rates, also represent combined elementary reactions including a unimolecular step followed by β scission. Rates of combined reactions of hydrogen abstraction and thermal decomposition are adjusted in the pre-factor to account for the number of all possible reactions according to the products.

Also, competing decomposition routes of cyclohexanes for benzene formation are proposed via cascading hydrogen abstraction followed by dehydrogenation reactions through the use of generic rates as illustrated in Fig. 2, by assumption that the hydrogen abstraction is the controlling step, with adjustments in statistical factors to account for the number of possible abstraction sites. For example, the generic rate is adjusted for hydrogen abstraction from methyl cyclohexane to account for the one hydrogen on the tertiary carbon and the ten other hydrogen atoms on the secondary carbons. Only the two most powerful hydrogen abstractors, H and OH radicals, are included and the intermediates and products are lumped to reduce the size of the extended mechanism. For example, all three isomers of methyl cyclohexene are represented by one species. Dehydrogenation of cyclohexanes gets more favorable as the ring becomes more unsaturated due to the emerging aromaticity.

4. Numerical results

Predicted concentrations of selected species using the Utah Surrogate Mechanism in three pre-

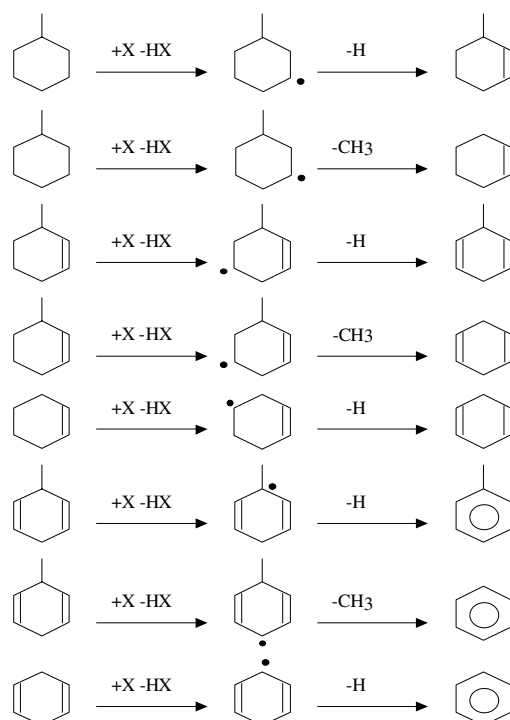


Fig. 2. Benzene formation routes from methyl cyclohexane. X = H, OH.

mixed flames of kerosene [1] ($P = 760$ torr, $\Phi = 1.7$), gasoline [2] ($P = 760$ torr, $\Phi = 1.0$) and natural gas [4] ($P = 40$ torr, $\Phi = 1.0$) are compared to experimental data in Figs. 3–5. The temperature profiles of these flames were shifted downstream in order to account for probe effects as discussed in detail elsewhere [21].

Because of the difficulty of following the fuel consumption in complex fuels, the predicted and measured consumption rates of oxygen are compared instead as shown in Fig. 3. The good agreement between predicted and measured concentrations for O_2 is also found for major products and important intermediates. Detailed comparisons between the measured and predicted concentration profiles of other species within the kerosene flame were reported elsewhere [3]. The predicted peak concentration of 1-pentene in the kerosene flame is within 5% of the measured value; those of 1-butene and di-acetylene are within 10%; those of ethylene and propylene are within 20%; those of acetylene, allene, and benzene within 30%; and those of *iso*-butene and methane within 50% of the experimental data.

The measured fuel consumption rate in the gasoline flame, represented by the profiles of major components of *iso*-pentane, iso-octane, and toluene in Fig. 4, is successfully reproduced.

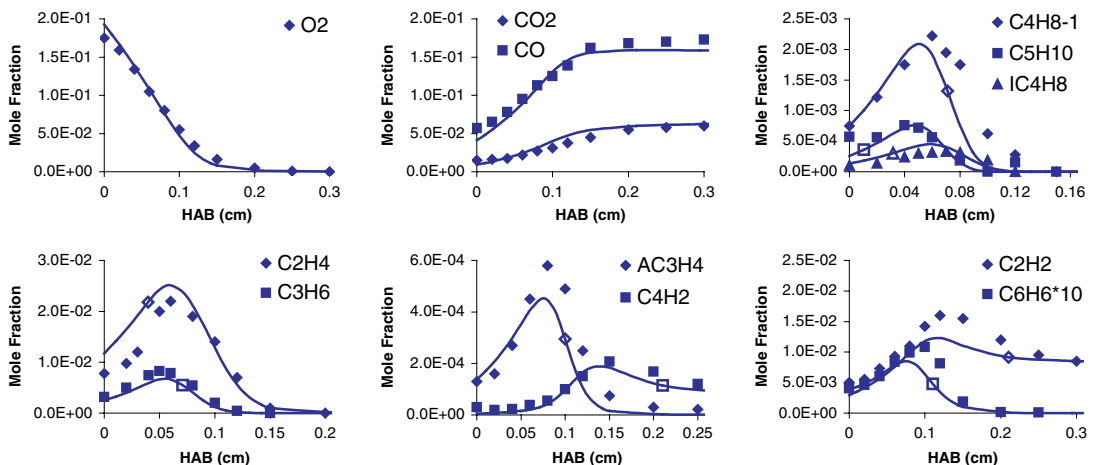


Fig. 3. Predicted and measured profiles of selected species in the kerosene flame [1]. The symbols represent the experimental data and the lines with symbol the simulations. HAB, height above burner.

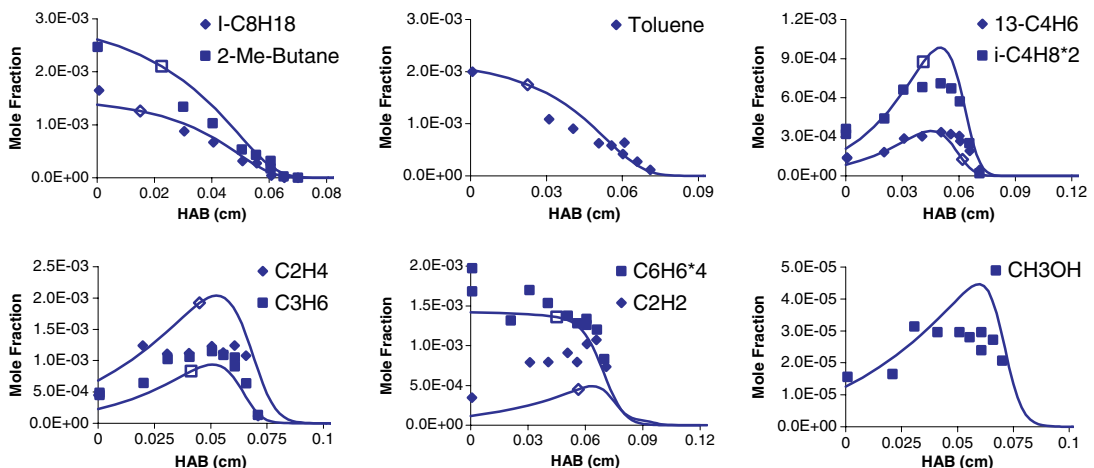


Fig. 4. Predicted and measured profiles of selected species in the gasoline flame [2]. The symbols represent the experimental data and the lines with symbol the simulations.

The predicted concentrations of major olefins are in good agreement with the experimental values. The peak concentration of propylene is under-predicted by 18.4% only. Those of ethylene and isobutene are over-predicted by 40–60%; however, the unexpected plateau in the profiles of these species makes it more difficult for the simulation to capture the experimental trend. A similar flat shape is observed in the concentration profile of methanol; the predicted concentrations of methanol are able to match the experimental data in the reaction zone only. The predicted benzene concentrations lie within the experimental uncertainties. The high concentration at the burner surface is a result of the benzene fraction in the fuel, and the simulation captures the unique feature of slow consumption of benzene due to the contribution

of cyclohexane dehydrogenation. The most successfully modeled species is probably 1,3-butadiene, the maximum concentration of which is over-predicted by 3.0% only. The maximum concentration of acetylene is under-predicted by a factor of two, likely due to the semi-detailed sub-mechanisms used for several major components other than the normal paraffin fractions.

The predicted and experimental concentrations of selected species in a natural gas flame are compared in Fig. 5. The fuel conversion rate has been well reproduced for the major components of methane, ethane and propane, and for the minor fractions of *n*-butane, *i*-butane, *n*-pentane, and *i*-pentane. It is noteworthy that the simulation is able to capture the experimental trends of slow consumption in the reaction zone for certain fuel

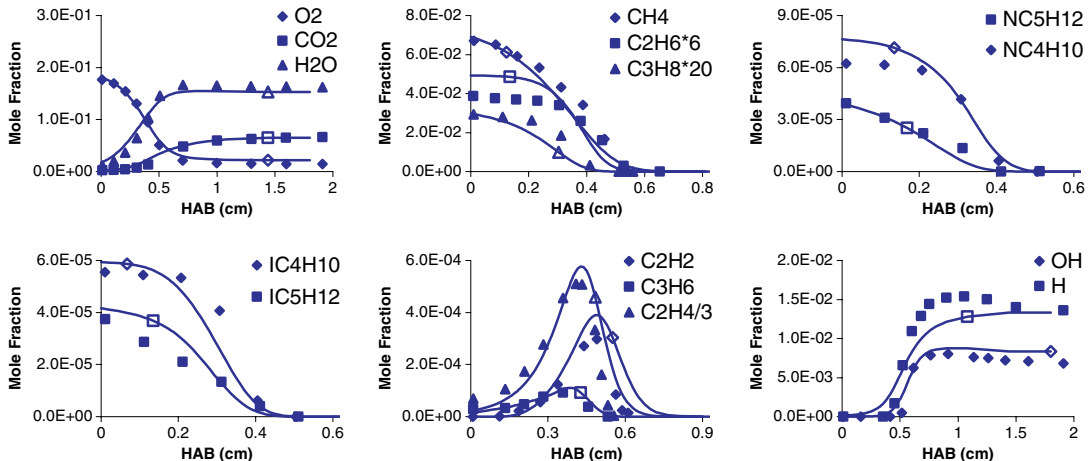


Fig. 5. Predicted and measured profiles of selected species in the natural gas flame [4]. The symbols represent the experimental data and the lines with symbol the simulations.

fractions, such as butanes, showing plateau shapes in the simulated concentration profiles of these components. The slower decomposition of butanes results from the formation of these species via the recombination of smaller C_1 to C_3 alkyl radicals that are abundant from the decomposition of major fuel components. The experimental concentrations of the oxidant and two major products of carbon dioxide and water vapor are almost perfectly reproduced, providing another evidence of the successful modeling of the fuel conversion rate in the flame. The predicted concentrations of olefins match the experimental profiles very well. For example, the predicted peak concentration of propylene is 18.4% higher than the measured value, with the peak position correctly estimated. The peak concentration of ethylene is also predicted well, and is only 13.1% higher than the experimental maximum. The measured profile of acetylene, one of the most important soot precursors, is also well reproduced, the peak concentration of which is over-predicted by 31.2%, with the position predicted correctly. The predicted concentrations of H and OH, the most important radicals, are in good agreement with the experimental profiles with the maximum deviations of 20% (H) and 10% (OH). This is a credit to the experimental results given the difficulty in measuring these species.

5. Discussion

The Utah Surrogate Mechanism has been validated for 41 flames of C_1 to C_{16} fuels, which include paraffins, olefins, acetylenes, oxygenates, and aromatics in this and previous work [3,21]. The maximum concentrations of benzene in 15 out of 22 flames, in which benzene concentration was measured, were predicted within 30% of the

experimental data. The major benzene formation pathways have been mapped out in flames burning a series of fuels, such as acetylenes, butadienes, and large *normal*-, *iso*- and *cyclo*-paraffins, which are major components of practical fuels [26]. The contributions of different constituents in a complex fuel to the total benzene formation, therefore, can be assessed by numerically modeling each constituent separately, in flames having a fixed equivalence ratio.

In Table 1, the predicted benzene concentrations in the kerosene flame are compared with those obtained in a series of modeled flames, burning an individual fuel component in each flame under the same experimental conditions (temperature profile included) except for the fuel composition. These modeled flames used the same equivalence ratio as the kerosene flame ($\Phi = 1.7$), with the N_2 mole fraction fixed. For example, the most important benzene producer besides the benzene fraction in the fuel is methyl cyclohexane. The benzene mole fraction in the methyl cyclohexane flame ($MCH/O_2/N_2 = 0.044/0.2719/0.6841$, $\Phi = 1.7$) reaches 4.14×10^{-3} at 0.0737 cm above the burner surface, compared to 7.45×10^{-5} obtained in the *n*-dodecane flame ($n-C_{12}H_{26}/O_2/N_2 = 0.0266/0.2893/0.6841$, $\Phi = 1.7$) at the same location. The predicted benzene concentrations in modeled naphthalene and substituted benzene flames are one order of magnitude higher than those obtained in *iso*-paraffin flames and are two orders of magnitude higher than those from *normal* paraffin flames. The predicted total concentration of C_5+ aromatic species in naphthalene flame is one order of magnitude higher than those obtained in *normal*- and *iso*-paraffin flames.

A rough estimation of the contribution from each individual component to soot precursor formation in the kerosene flame and the sum of these

Table 1

Soot precursor production potentials of individual fuel components

Height above burner (cm)	Normal C ₁₂ H ₂₆	Iso C ₈ H ₁₈	Methyl cycloC ₆	C ₆ H ₅ CH ₃	C ₆ H ₆	Full surrogate
Benzene concentration (ppm) at $\Phi = 1.7, P = 1 \text{ atm}$						
0.0211	22.9	66.6	1300	794	47700	485
0.0737	74.5	226	4140	2620	28400	850
0.1	76.2	316	3700	3860	17800	638
Acetylene concentration (ppm) at $\Phi = 1.7$						
0.1158	13400	10100	10900	7000	10300	12300
C_5^+ aromatic species concentration (ppm) at $\Phi = 1.7$						
0.0737	208	566	5490	38500	34800	2300

contributions are presented in Table 2, obtained by using the sum of the predicted benzene concentrations of each component in modeled flames weighed by the molar percent of this component in the kerosene surrogate. The estimation was compared with results obtained using the surrogate fuel (last column in Table 1). The estimated sum roughly reproduces the measured benzene concentration in the kerosene flame with deviations of +20–60%, and overestimates the total C_5^+ aromatic concentration by a factor of two. The overestimation is a consequence of the substantial production from modeled aromatics flames, and implies the catalytic effects on the decomposition of aromatic species when paraffinic species are presented in flames, due to enhanced formation of radicals. The naphthalene and aromatic fractions yield benzene and C_5^+ aromatic concentrations about one order of magnitude greater than those obtained from paraffin fractions.

In contrast, acetylene formation is not sensitive to fuel structure; acetylene concentration is highest in the flame of *n*-dodecane (Table 1), with a value only twice that in the toluene flame and comparable to those in the flames of other components. More interestingly, the sum of the weighted the acetylene concentrations derived from five modeled flames (12,298 ppm) estimates the acetylene concentration through the use of the full surrogate (12,300 ppm) almost exactly. Acetylene concentrations in a practical fuel, therefore, very

likely can be estimated from those obtained, via experiments or simulations, in flames of representative chemical compounds under similar conditions.

6. Conclusions

A new mechanism was generated and extended to describe three common composite fuels, and was validated with data obtained over a range of equivalence ratios from 1.0 to 1.7. Mechanism generation through the use of generic rates has greatly reduced the mechanism generation effort, and proved to be successful as seen in the comparison between the calculated and measured concentrations, which include those of soot precursors, for composite fuels containing high concentrations of paraffins. The ability to predict the formation of soot precursors such as acetylene and benzene is one of the major contributions of the present paper. The relative tendency of each component to form soot precursors can guide the formulation of future fuels that produce less soot, which is desirable in combustors such as gas turbines. Results reported in Tables 1, 2 infer strong precursor production potential of certain fuel fractions in liquid transportation fuels. The importance of naphthalene and aromatic fractions in benzene formation is clear, although these fractions account for only

Table 2

Contributions of individual fuel components to soot precursor formation

Height above burner (cm)	<i>n</i> -C ₁₂ H ₂₆	<i>i</i> -C ₈ H ₁₈	CH ₃ -cycloC ₆	C ₆ H ₅ CH ₃	C ₆ H ₆	Sum
Mole %	73.5	5.5	10	10	1	100
Benzene concentration (ppm) \times fuel fraction						
0.0211	16.8	3.7	130	79.4	477	707
0.0737	54.8	12.4	414	262	284	1027
0.1	56.0	17.4	370	386	178	1007
Acetylene concentration (ppm) \times fuel fraction						
0.1158	9849	556	1090	700	103	12298
C_5^+ aromatic species concentration (ppm) \times fuel fraction						
0.0737	153	31	549	3850	348	4931

20% of the surrogate. In contrast, the flames of each individual component in the kerosene produce similar amounts of acetylene. In the formulation of surrogate fuels to simulate soot formation, major attention should be given to the components leading to benzene formation, an important species in particle nucleation and surface condensation, since the formation of acetylene, the addition of which dominates soot surface growth, is relatively insensitive to fuel composition. Interestingly, the findings support the generalization that the propensity for benzene formation in this study is consistent with the generalization that soot propensity of fuel components is given by aromatics > cyclo-paraffins > *i*-paraffins > *n*-paraffins.

Acknowledgments

This research was funded by the University of Utah (C-SAFE), through a contract with the Department of Energy, Lawrence Livermore National Laboratory (B341493).

Appendix A. Supplementary data

Supplementary data associated with this article can be found in the online version at doi:10.1016/j.proci.2006.08.001.

References

- [1] C. Doute, J.-L. Delfau, R. Akrich, C. Vovelle, *Combust. Sci. Technol.* 106 (4-6) (1995) 327–344.
- [2] A. Hakansson, K. Stromberg, J. Pedersen, J.O. Olsson, *Chemosphere* 44 (5) (2001) 1243–1252.
- [3] H. Zhang, Ph.D. dissertation, the Department of Chemical Engineering, the University of Utah, May, 2005.
- [4] A. Turbiez, A. El Bakali, J.F. Pauwels, A. Rida, P. Meunier, *Fuel* 83 (7–8) (2004) 933–941.
- [5] H.J. Curran, P. Gaffuri, W.J. Pitz, C.K. Westbrook, *Combust. Flame* 114 (1998) 149–177.
- [6] J.M. Simmie, *Prog. Energy Combust. Sci.* 29 (6) (2003) 599–634.
- [7] E. Ranzi, M. Dente, A. Goldenig, G. Bozzano, T. Faravelli, *Prog. Energy Combust. Sci.* 27 (1) (2001) 99–139.
- [8] C. Bales-Gueret, M. Cathonnet, J.C. Boettner, F. Gaillard, *Energy Fuels* 6 (2) (1992) 189–194.
- [9] M. Cathonnet, P. Dagaut, A. Chakir, J.C. Boettner, *Trends Phys. Chem.* 1 (1) (1990) 167–178.
- [10] P. Dagaut, M. Reuillon, J.C. Boettner, M. Cathonnet, *Proc. Combust. Inst.* 25 (1994) 919–926.
- [11] J.L. Delfau, M. Bouhria, M. Reuillon, O. Sanogo, R. Akrich, C. Vovelle, *Proc. Combust. Inst.* 23 (1990) 1567–1572.
- [12] C. Vovelle, J.L. Delfau, M. Reuillon, in: H. Bockhorn (Ed), *Soot Formation in Combustion*, Springer Series in Chemical Physics 59, 1994, p. 50.
- [13] C. Doute, J.L. Delfau, R. Akrich, C. Vovelle, *Combust. Sci. Technol.* 106 (4-6) (1995) 327–344.
- [14] R. Fournet, F. Battin-Leclerc, P.A. Glaude, B. Judenherc, V. Warth, G.M. Come, G. Scacchi, A. Ristori, G. Pengloan, P. Dagaut, M. Cathonnet, *Int. J. Chem. Kinet.* 33 (10) (2001) 574–586.
- [15] F. Battin-Leclerc, R. Fournet, P.A. Glaude, B. Judenherc, V. Warth, G.M. Come, G. Scacchi, *Proc. Combust. Inst.* 28 (2000) 1597–1605.
- [16] P.A. Glaude, V. Warth, R. Fournet, F. Battin-Leclerc, G. Scacchi, G.M. Come, *Int. J. Chem. Kinet.* 30 (12) (1998) 949–959.
- [17] A.G. Kyne, P.M. Patterson, M. Pourkashanian, A. Williams, C.W. Wilson, in: *Proc. International Symposium on Air Breathing Engines*, 14th, Florence, Italy, September 5–10, 1999, pp. 377–387.
- [18] M.A. Mawid, T.W. Park, B. Sekar, C. Arana, 713 26th JANNAF Airbreathing Propulsion Subcommittee Meeting, vol. 1, 2002, pp. 21–37.
- [19] C. Doute, J.L. Delfau, C. Vovelle, *Combust. Sci. Technol.* 130 (1–6) (1997) 269–313.
- [20] G. Bikas, N. Peters, *Combust. Flame* 126 (1/2) (2001) 1456–1475.
- [21] H.R. Zhang, E.G. Eddings, A.F. Sarofim, *Combust. Sci. Technol.* (2006) (in press).
- [22] H.R. Zhang, L.K. Huynh, N. Kungwan, S. Zhang, Z. Yang, T.N. Truong, E.G. Eddings, A.F. Sarofim, *Preprints of Symposia—American Chemical Society, Division of Fuel Chemistry* 51 (1) (2006) 229–231.
- [23] R.J. Kee, F.M. Rupley, J.A. Miller, et al., Chemkin Collection, Release 4.0, Reaction Design, Inc, San Diego, CA, 2004.
- [24] S. Yan, E.G. Eddings, A.B. Palotas, R.J. Pugmire, A.F. Sarofim, *Energy Fuels* 19 (16) (2005) 2408–2415.
- [25] A. Violi, S. Yan, E.G. Eddings, A.F. Sarofim, S. Granata, T. Faravelli, E. Ranzi, *Combust. Sci. Technol.* 174 (2002) 399–417.
- [26] H.R. Zhang, E.G. Eddings, A.F. Sarofim, *Preprints of Symposia—American Chemical Society, Division of Fuel Chemistry* 51 (1) (2006) 351–352.

Comment

Robert J. Santoro, Penn State University, USA. Have you compared your kinetic chemical reaction results with an equilibrium calculation for the fuel mixture?

Reply. This question was targeted to the predictions summarized in Table 1. The equilibrium concentrations for acetylene and benzene under these conditions are

much lower than the values predicted by the kinetic model for the surrogate mixture, as well as for the individual surrogate components. Thus, we are far from equilibrium at these conditions.

It is interesting to note that while the H/C ratios for normal-, iso- and cyclo-paraffins are approximately the same, and thus would produce similar equilibrium

levels, there were significant differences among the benzene and aromatic concentrations predicted for pre-mixed flames of these fuels, which would indicate a

kinetically controlled structural effect on the formation of aromatics. Such an effect was not observed for acetylene formation.